

Bromine atom diffusion on stepped and kinked copper surfaces

D.M. Rampulla, A.J. Gellman, David S. Sholl *

Department of Chemical Engineering, Carnegie Mellon University, Pittsburgh, PA 15213, USA

Received 23 November 2005; accepted for publication 8 March 2006

Available online 29 March 2006

Abstract

The rates of Br atom diffusion on several single crystalline Cu surfaces have been studied because of the potential impact of Br diffusion on the selectivity of alkyl bromide surface chemistry on Cu. Density functional theory (DFT) has been used to study the diffusion of isolated bromine atoms on a flat Cu surface, Cu(111), two Cu surfaces with straight steps, Cu(221) and Cu(533), and two kinked Cu surfaces, Cu(643) and Cu(531). Bromine diffusion is rapid on the flat Cu(111) surface with a barrier of $\Delta E_{\text{diff}} = 0.06$ eV and a hopping frequency of $\nu = 4.8 \times 10^{10} \text{ s}^{-1}$ at 150 K. On the stepped and kinked surfaces the effective diffusion barriers lie in the range $\Delta E_{\text{diff}} = 0.18$ – 0.31 eV. Thus the rates of diffusion are many orders of magnitude slower on stepped and kinked Cu surfaces than on the Cu(111) surface. Nonetheless, at temperatures relevant for alkyl bromide debromination on Cu surfaces, bromine atoms remain sufficiently mobile that they can explore all available binding sites on the timescale of the debromination reaction.

© 2006 Elsevier B.V. All rights reserved.

Keywords: Copper; Alkyl bromides; DFT; Diffusion; Surfaces

1. Introduction

A variety of fundamental and applied applications of metal surfaces involve the presence of adsorbed halide atoms. Organo-halides are frequently used as precursors to the formation of adsorbed organic groups on metal surfaces [1,2]. Experiments of this type typically probe the properties of the resulting organic groups in the presence of coadsorbed halides because the latter species adsorb strongly to metals. Some examples exist suggesting that the presence of adsorbed halides can have an important influence on the surface chemistry available to coadsorbed species. In one example, Jenks et al. observed that clustering of iodine atoms on Cu(110) and Cu(100) surfaces inhibited β -hydride elimination [3]. Recently, bromine clustering has been found to be responsible for inhibiting β -hydride elimination on kinked, high Miller index Cu surfaces [4,5]. In some instances, the presence of coadsorbed halides can be used to design experiments that selectively probe

particular surface sites. Adsorption of halogens has been used for this purpose as a means of selectively blocking surface defect sites such as kinks and steps to distinguish between the contributions to molecular desorption from terrace, step and kink sites [6,7]. In a more applied context, adsorbed halides are also known to act as promoters for some catalytic reactions. For example, Cl is a useful promoter for Ag-catalyzed ethylene epoxidation [8,9].

To fully understand the role of adsorbed halides in each of the settings listed above, it is necessary to characterize the preferred sites for halide adsorption on metal surfaces at equilibrium and the rate at which these preferred sites will become occupied once halides are present. Although DFT calculations have predicted that the activation energies for adsorbed I and Br on flat metal surfaces are small (that is, less than 0.25 eV) [7,10], little information is available about the diffusion processes of halides on more complex surfaces. Since it is likely that halide atoms adsorb considerably more favorably at step and defect sites than on atomically flat terraces on metals, it is possible that the presence of step edges could radically reduce the diffusion rates of adsorbed halides relative to surface terraces. The magnitude of this effect is relevant to all situations that

* Corresponding author. Tel.: +1 412 268 4207; fax: +1 412 268 7139.
E-mail address: sholl@andrew.cmu.edu (D.S. Sholl).

involve halide adsorption on metals, but it is particularly important for experiments that use alkyl halides as part of an effort to characterize the adsorption or chemistry of small organic species on stepped surfaces [6,7]. If the diffusion of halide atoms on these surfaces is extremely slow, great care would need to be taken in interpreting the outcomes of these experiments in terms of the equilibrium distribution of halides among the adsorption sites available to them.

In this paper, we examine a specific example of halide diffusion on stepped metal surfaces, namely Br diffusion on stepped Cu surfaces vicinal to Cu(111), to develop some initial information pertinent to the broader issue of halide surface diffusion rates. We have used density functional theory (DFT) to study the diffusion of isolated Br adatoms on Cu(111), two surfaces with straight steps and (111)-oriented terraces, Cu(221) and Cu(533), and a kinked surface with a (111) oriented terrace, Cu(643), and Cu(531). This specific set of surfaces is of interest because it includes the class of intrinsically chiral surfaces that has been studied experimentally in the greatest detail [6,11–13]. We expect that obtaining results for a series of surfaces like this will also give a useful framework for predicting the general properties of adsorbed halides on similar surfaces. Calculations of this type cannot provide a complete description of the influence of adsorbed halides on the chemistry of these surfaces, since they do not consider the possibility of halide atom clustering or the competition between halides and other chemisorbed species for surface sites. Nevertheless, describing the properties of isolated adatoms is a necessary prerequisite for considering these more complex issues.

2. Calculation details

DFT calculations were performed using VASP [14]. The Vanderbilt Ultrasoft Pseudopotential [15,16] was selected for use from the VASP pseudopotential database [15–17]. Electron exchange–correlation effects were described by the Generalized Gradient Approximation (GGA) using the Perdew–Wang 91 functional. All calculations used a plane wave expansion with a cutoff energy of 233.7 eV. A Monkhorst–Pack mesh with a $4 \times 4 \times 1$ k -point grid was used for the calculations on Cu(643), a $5 \times 5 \times 1$ k -point grid was used for the calculations on Cu(111) and Cu(531), and a $6 \times 6 \times 1$ k -point grid was used for the calculations on Cu(221) and Cu(533). Preliminary calculations indicated that these k -space samplings were well converged. A DFT-optimized lattice constant of 3.64 Å was used for Cu. The Br adatoms and the Cu atoms in the upper two layers of the Cu(111) supercell were allowed to relax. For calculations with stepped and kinked surfaces, the Br adatoms and the Cu atoms forming the physical surface were allowed to relax. Structures were relaxed using a quasi-Newton algorithm until the forces on all the unconstrained atoms were <0.03 eV/Å. A vacuum spacing of ~ 4 –5 (111) layer spacings was used to separate the peri-

odic slabs for all surfaces in the direction of the surface normal.

The adsorption energies, ΔE_{ads} , of the Br adlayers were defined based on the dissociative adsorption of Br₂:

$$\Delta E_{\text{ads}} = \left(E_{\text{Cu}} + \frac{1}{2} E_{\text{Br}_2} - E_{\text{Br,ads}} \right).$$

The total energy of the bare Cu surface is E_{Cu} ; the total energy of gaseous bromine is E_{Br_2} ; and the total energy of the Cu surface with the Br adlayer is $E_{\text{Br,ads}}$. With this definition, an increasing value of adsorption energy indicates a stronger bond between the Br atom and the Cu surface.

The diffusion barrier between two adjacent adsorption sites was determined using the Nudged Elastic Band (NEB) method developed by Jónsson and co-workers [18–20] to find the energy maximum along the minimum energy path (MEP) between the two sites. NEB calculations were performed for hops between adjacent local minima for which the MEP could initially be approximated by linear interpolation. In most cases, multiple hops were then combined to provide the final MEP. For the Cu(111) surface, five images were relaxed between the fixed initial and the final states. For Cu(221), 11 images were relaxed between the fixed initial and the final states to determine half of the MEP. Due to symmetry along the path, the other half of the MEP was simply the reverse of the path determined by the original 11 images. For Cu(533), 23 images were relaxed between the fixed initial and the final states. For Cu(643) and Cu(531), the final MEPs contained 29 and 17 images, respectively. In each case, the diffusion barrier, ΔE_{diff} , was taken to be the difference between the maximum and the minimum energies along the final MEP.

After finding the diffusion barrier, hopping frequencies, ν , were approximated by [21]

$$\nu = \nu_0 \exp(-\Delta E_{\text{diff}}/k_{\text{B}}T),$$

where ν_0 , was taken to be 5×10^{12} s⁻¹ [10], k_{B} is the Boltzmann constant, and T is temperature. In reporting these approximate hopping frequencies, we used $T = 150$ K, which is the approximate temperature of alkyl bromide debromination on Cu surfaces [22].

3. Results and discussion

3.1. Br diffusion on Cu(111), Cu(221), and Cu(533)

Br diffusion was initially studied on the atomically flat Cu(111) surface. The Br adlayer coverage was 0.11 ML (1 ML = 1 adatom per surface Cu atom). Our DFT calculations used the (3 × 3) surface unit cell shown in Fig. 1. The strongest binding occurred at the fcc and hcp threefold hollow sites with adsorption energies of 1.77 eV. The two-fold bridge site is a transition state for Br diffusion between adjacent threefold sites. Adsorption of Br in an on-top site yields a second-order saddle with a binding energy that is 0.35 eV lower than the favored threefold sites. The diffusion barrier for Br hopping between fcc and hcp sites is

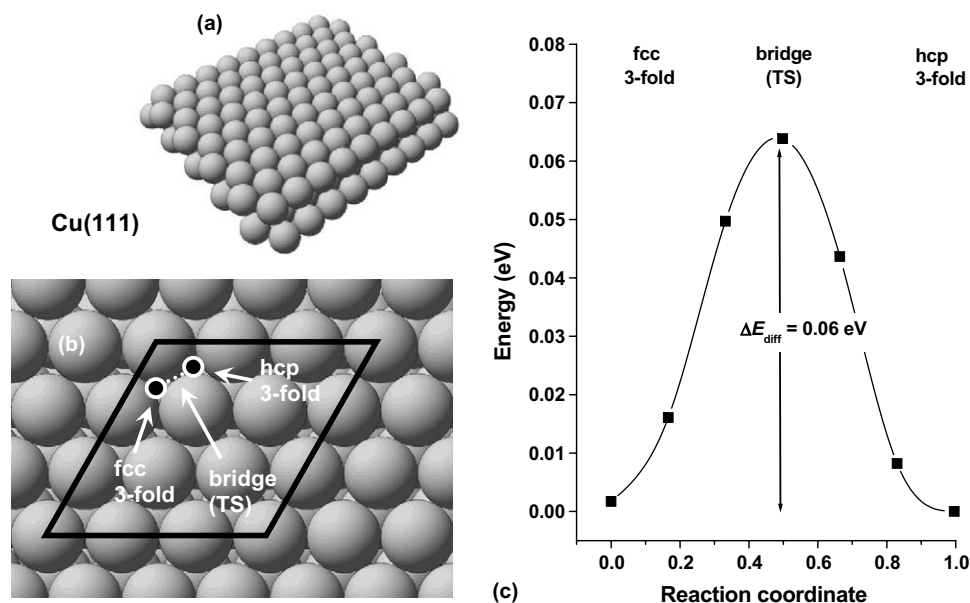


Fig. 1. (a) The structure of the Cu(111) surface; (b) the unit cell used for diffusion calculations and (c) the bromine adsorption energy along the MEP connecting an fcc hollow site with an hcp hollow site. The thick, dark line in (b) outlines the computational supercell used in the calculations. The points (●) mark the initial and final states of the MEP (dotted white line). The transition state occurs with a barrier of $\Delta E_{\text{diff}} = 0.06 \text{ eV}$ and is located at the bridge site between the fcc threefold hollow site and the hcp threefold hollow site.

$\Delta E_{\text{diff}} = 0.06 \text{ eV}$. This value is close to the diffusion barrier of 0.04 eV predicted by DFT for I on Cu(111) [7]. The approximate hopping frequency for Br diffusion on Cu(111) is $\nu = 4.8 \times 10^{10} \text{ s}^{-1}$ at 150 K.

To probe the diffusion of Br on stepped Cu surfaces, we first examined the Cu(221) and Cu(533) surfaces, which have straight steps. Cu(221) and Cu(533) both have (111)-oriented terraces that are three atoms wide and separate monoatomic surface steps. The two surfaces differ in the local structure of the surface step edges. On Cu(221) the step edge is a (110) microfacet, while on Cu(533) the step edge is a (100) microfacet. To perform calculations with a similar surface coverage to that used on the Cu(111) surface, a (1×3) surface unit cell was used for both Cu(221) and Cu(533). These unit cells are illustrated in Figs. 2 and 3, respectively. This yields a Br adlayer of 0.10 ML on Cu(221) and 0.09 ML on Cu(533), where 1 ML is equivalent to one adatom per surface Cu atom. Many binding sites on the terraces and step edges were examined on both stepped surfaces, revealing that the strongest adsorption occurred along the step edge.

The strongest binding site on Cu(221) is the hcp threefold hollow closest to the step edge which has an adsorption energy of $\Delta E_{\text{ads}} = 1.89 \text{ eV}$. The fcc threefold sites on the terrace above the step edge, denoted 'A' in Fig. 2, have binding energies that are 0.16 eV less favorable than the hcp threefold sites that lie along the step edge. Adsorption on threefold sites in the middle of the terrace is $>0.4 \text{ eV}$ less favorable than the most stable step edge site. Br can also bind below the step edge, but the energy of these sites is 0.10 eV less favorable than binding on top of the step edge. This observation is similar to the behavior of O on stepped

Pt surfaces, where the passivation of step edge atoms by adsorption makes binding sites on top of the step edge preferred over binding of the electronegative adsorbate in the more electron rich sites at the base of the steps [23].

Fig. 2 shows the MEP for Br diffusion on Cu(221). The initial and final states of the path are bridge sites between atoms along the step edge. These sites are local minima, but are separated from the slightly more stable hcp edge sites by only a tiny energy barrier; therefore, the bridge-edge sites do not significantly contribute to the complete MEP. The fcc site labeled 'A' that lies along the MEP is a local minimum between the two stable hcp sites that lie along the step edge. As might be expected from the results obtained on Cu(111), Br diffuses along the top of the Cu(221) step edge by hopping between adjacent hcp and fcc sites. The net diffusion barrier for motion along the step edge is $\Delta E_{\text{diff}} = 0.18 \text{ eV}$, which is three times larger than the diffusion barrier on Cu(111). A value of $\Delta E_{\text{diff}} = 0.18 \text{ eV}$ corresponds to an approximate hopping frequency of $\nu = 4.5 \times 10^6 \text{ s}^{-1}$ at 150 K. Because the hopping rate out of the local minimum at site 'A' on the terrace is much larger than this approximate hopping frequency, $\nu = 4.5 \times 10^6 \text{ s}^{-1}$ is a reasonable approximation for the frequency of hops between adjacent hcp hollow sites along the Cu(221) step edge.

There are subtle differences between Br diffusion on the Cu(221) and Cu(533) surfaces. On Cu(533) the strongest binding occurred with an adsorption energy of $\Delta E_{\text{ads}} = 1.91 \text{ eV}$ at the bridge site between the atoms along the step edge. The MEP for Br diffusion along the Cu(533) step edge is shown in Fig. 3. On this surface the hcp threefold site, which is separated from the step edge by a single Cu

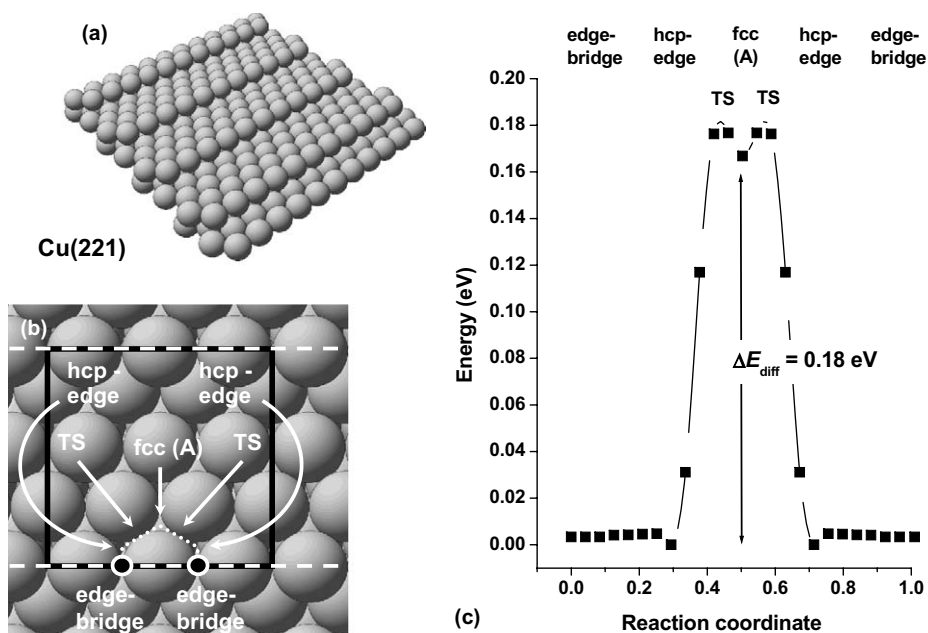


Fig. 2. (a) The structure of the Cu(221) surface; (b) the unit cell used for diffusion calculations and (c) the bromine adsorption energy along the MEP connecting equivalent bridging sites at the step edge. The thick, dark line in (b) outlines the computational supercell used in the calculations. The points (●) mark the initial and final states of the MEP (dotted white line). The MEP includes a local minimum at the fcc threefold hollow that lies one atom from the step edge. The transition state occurs with a barrier of $\Delta E_{\text{diff}} = 0.18$ eV and is located at the bridge site between the fcc threefold hollow site and the step edge bridging site.

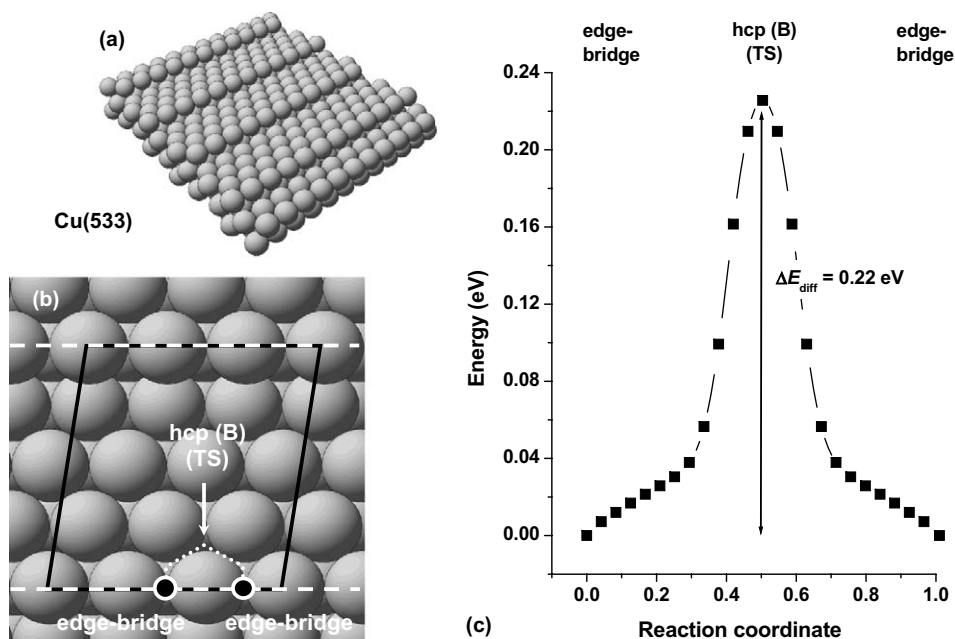


Fig. 3. (a) The structure of the Cu(533) surface; (b) the unit cell used for diffusion calculations and (c) the bromine adsorption energy along the MEP connecting equivalent bridging sites at the step edge. The thick, dark line in (b) outlines the computational supercell used in the calculations. The points (●) mark the initial and final states of the MEP (dotted white line). The transition state occurs with a barrier of $\Delta E_{\text{diff}} = 0.22$ eV and is located at the hcp threefold hollow lying one atom from the step edge.

atom, is not a local minimum as it is on Cu(221). Instead it is the transition state for diffusion along the step edge. The diffusion barrier is $\Delta E_{\text{diff}} = 0.22$ eV, which is slightly larger than the diffusion barrier on Cu(221) and yields an approximate hopping frequency of $\nu = 2.0 \times 10^5 \text{ s}^{-1}$ at 150 K.

3.2. Br diffusion on Cu(643) and Cu(531)

The Cu(643) surface has kinked-stepped edges separated by (111)-oriented terraces (Fig. 4). High Miller index surfaces of this type are of great interest because they are intrinsically chiral [6,11,12,24]. They also provide models

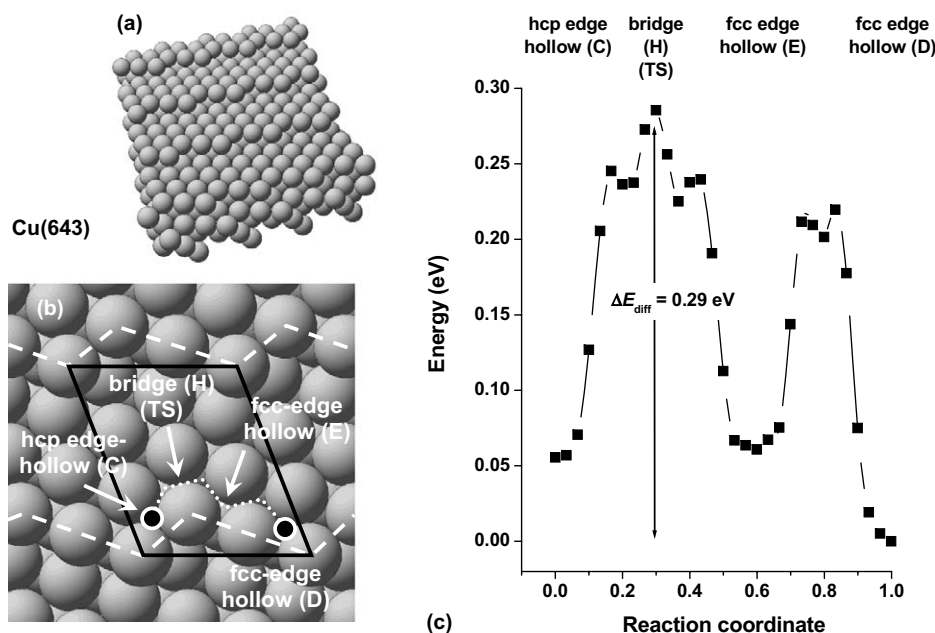


Fig. 4. (a) The structure of the Cu(643) surface; (b) the unit cell used for diffusion calculations and (c) the bromine adsorption energy along the MEP connecting hollow sites at the step edge. The thick, dark line in (b) outlines the computational supercell used in the calculations. The points (●) mark the initial and final states of the MEP (dotted white line) leading from site ‘C’ to site ‘D’. There are several local minima along the MEP including a deep local minimum at the fcc threefold hollow adjacent to the long step edge. The transition state occurs with a barrier of $\Delta E_{\text{diff}} = 0.29$ eV and is located at the bridging site adjacent to the kink.

of surface defects that are well-suited for plane wave DFT calculations [7,13,25–28]. On Cu(643) the terrace is three atoms wide. The long step edge is formed by a (100) microfacet that is two atoms long. The short step edge or kink is formed by a (110) microfacet that is one atom wide. On Cu(531) one cannot define terrace, step and kinks sites because the three low Miller index microfacets exposed at the surface each span just one unit cell width (Fig. 5). All calculations were performed for the ideal terminations of Cu(643) and Cu(531), although we note in this context that in reality the step edges of high Miller index Cu surfaces exhibit considerable disorder at elevated temperatures [29,30]. Our DFT calculations used a single surface unit cell for each surface, corresponding to a Br coverage of 0.11 ML on Cu(643) and 0.29 ML on Cu(531), where 1 ML = 1 adatom per surface Cu atom. The Cu(643) supercell is shown in Fig. 4, and the Cu(531) supercell is shown in Fig. 5. Many binding sites on the terraces and kinked step edges were examined on both Cu(643) and Cu(531), but as with the surfaces having straight steps, the strongest adsorption sites occurred along the step edge.

The strongest binding on Cu(643) occurred at the hcp hollow site denoted ‘D’ in Fig. 4, which is located adjacent to the kink and has an adsorption energy of $\Delta E_{\text{ads}} = 1.98$ eV. The fcc threefold site denoted ‘C’ in Fig. 4 is slightly less favored, with an adsorption energy that is 0.05 eV less than that of site ‘D’. Fig. 4 shows the calculated MEP for Br diffusion on Cu(643) for diffusion from site ‘C’ to site ‘D’. Diffusion occurs via a series of hops between adjacent threefold sites. There are six distinct local

minima along the MEP, including the initial and final states. From site ‘C’ to the stable site at the reaction coordinate of 0.6 (see Fig. 4c) the hopping frequency is $\nu = 4.3 \times 10^4 \text{ s}^{-1}$. From the stable site at the reaction coordinate of 0.6 to site ‘C’ the hopping frequency is $\nu = 9.4 \times 10^4 \text{ s}^{-1}$. From the stable site at the reaction coordinate of 0.6 to site ‘D’ the hopping frequency is $\nu = 2.1 \times 10^7 \text{ s}^{-1}$. From site ‘D’ to the stable site at the reaction coordinate of 0.6 the hopping frequency is $\nu = 2.0 \times 10^5 \text{ s}^{-1}$. The diffusion-limiting transition state occurs at the bridge site denoted ‘H’ in Fig. 4, and the estimated hopping frequency for net hops from ‘D’ to ‘C’ along the reaction coordinate shown in Fig. 4 is $\nu = 9.0 \times 10^2 \text{ s}^{-1}$. We did not compute the activation energy for a direct hop from site ‘C’ to site ‘D’ across the boundary of the unit cell marked in Fig. 4, as the results above strongly suggest that this barrier will not be rate limiting for net diffusion.

The strongest binding on Cu(531) occurred at the hollow-edge ‘Z’ site with an adsorption energy of $\Delta E_{\text{ads}} = 1.87$ eV and the hollow-edge ‘W’ site with an adsorption energy of $\Delta E_{\text{ads}} = 1.86$ eV. Fig. 5 shows the calculated MEP for Br diffusion between these two sites on Cu(531). Although there are several local minima along the MEP, the rate-determining transition state is clearly the one associated with the threefold hollow ‘Y’. The fact that this site is a transition state rather than a local minimum is similar to the situation on Cu(533). The net diffusion barrier is $\Delta E_{\text{diff}} = 0.31$ eV, which is similar to the diffusion barrier on Cu(643). The hopping frequency associated with this barrier is $\nu = 1.9 \times 10^2 \text{ s}^{-1}$, and it is

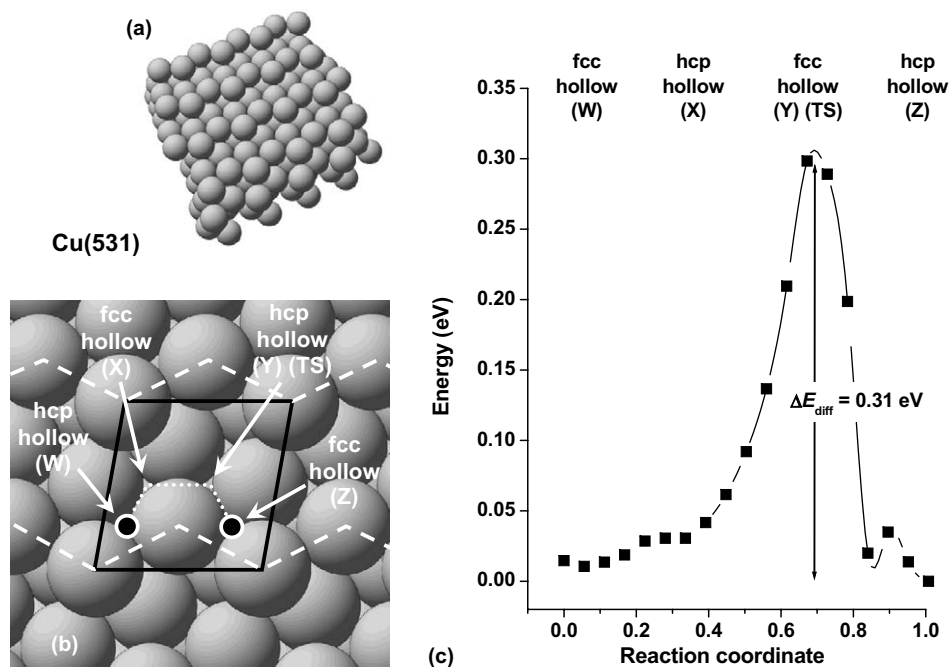


Fig. 5. (a) The structure of the Cu(531) surface; (b) the unit cell used for diffusion calculations and (c) the bromine adsorption energy along the MEP connecting hollow sites at the step edge. The thick, dark line in (b) outlines the computational supercell used in the calculations. The points (●) mark the initial and final states of the MEP (dotted white line) leading from site ‘W’ to site ‘Z’. The transition state occurs with a barrier of $\Delta E_{\text{diff}} = 0.31$ eV and is located at the fcc hollow marked ‘Y’.

reasonable to think of this frequency as being associated with motion along the entire MEP shown in Fig. 5. We did not compute the energy barrier for the direct pathway from site ‘Z’ to site ‘W’, because it appears extremely unlikely that this barrier will be rate limiting for net diffusion along the step edge.

4. Conclusions

Our DFT calculations have estimated the activation energies required for diffusion of isolated Br atoms on flat and stepped Cu surfaces with (111)-oriented terraces. As might be qualitatively expected, the adsorption energies and diffusion barriers of Br atoms are higher on stepped and kinked Cu surfaces than on the atomically flat Cu(111) surface. On all the high Miller index surfaces examined, the strongest binding sites occurred along the top of the step edge. The minimum energy paths for diffusion on the four stepped surfaces all follow the step edge, via a series of hops between stable edge bridge and threefold sites. We estimated the hopping rates of Br on each surface at 150 K, a temperature relevant to debromination reactions of alkyl bromides on Cu surfaces. The slowest diffusion occurred on the kinked-stepped Cu(643) and Cu(531) surfaces; diffusion on the straight stepped surfaces and on Cu(111) is several orders of magnitude faster. Even on the kinked-stepped surfaces, however, diffusion is sufficiently rapid that it is clearly valid to assume that adsorbed Br atoms on Cu surfaces with (111)-oriented terraces will reach thermodynamic equilibrium under experimental conditions.

It is interesting to consider how well the conclusions of our calculations might be generalized to other halides or other surface orientations. The binding sites favored by Br and the diffusion activation energy for Br on Cu(111) are similar to those calculated previously for isolated iodine atoms [7]. This observation suggests that it is reasonable to predict that the diffusion of halogens other than Br on stepped Cu surfaces with (111)-oriented terraces will also be relatively rapid. It is not as clear that this conclusion can be extended to stepped Cu surfaces with terraces that are not (111)-oriented. The diffusion activation energy calculated for Br diffusion on the kinked steps of Cu(643) is slightly larger than an earlier DFT calculation for the diffusion of Br on atomically flat Cu(100) [10]. Despite this apparent structure sensitivity, there is no suggestion from any of the calculated diffusion activation energies that the diffusion of Br or any other halide on Cu surfaces will be so slow as to strongly limit the ability of adsorbed halides to reach equilibrium on time scales relevant to most experiments.

An important limitation in our calculations is that we have only considered the diffusion of Br on Cu surfaces with ideally terminated Miller index surface structures. We have not examined possible scenarios in which the presence of Br atoms induces surface restructuring. Scenarios of this type have been suggested as possible explanations for results observed in STM experiments with Br on Cu(100) [10]. The structure of real kinked-stepped surfaces is considerably more complex than the ideal terminations used in our DFT calculations because of thermally-induced

disorder in the step edges [29,30]. Our calculations reveal that Br binds with slightly higher energies at step-kink sites than on straight step edges on Cu surfaces with (111)-oriented terraces. This suggests that the presence of adsorbed Br on surfaces of this type may increase the equilibrium density of kinks on real stepped Cu surfaces.

Acknowledgements

This research was supported by the MRSEC program of the NSF under Award No. DMR-0079996 and by NSF Grant CTS-0216170.

References

- [1] A.J. Gellman, J. Phys. Chem. B 106 (2002) 10509.
- [2] S. Linic, M.A. Barteau, J. Am. Chem. Soc. 124 (2002) 310.
- [3] C.J. Jenks, A. Paul, L.A. Smoliar, B.E. Bent, J. Phys. Chem. 98 (1994) 572.
- [4] D.M. Rampulla, A.J. Francis, K.S. Knight, A.J. Gellman, J. Phys. Chem. B, submitted for publication.
- [5] D.M. Rampulla, A.J. Gellman, Surf. Sci., submitted for publication.
- [6] J.D. Horvath, A. Koritnik, P. Kamakoti, D.S. Sholl, A.J. Gellman, J. Am. Chem. Soc. 126 (2004) 14988.
- [7] P. Kamakoti, J. Horvath, A.J. Gellman, D.S. Sholl, Surf. Sci. 563 (2004) 206.
- [8] S. Linic, M.A. Barteau, J. Catal. 214 (2003) 200.
- [9] S. Linic, M.A. Barteau, J. Am. Chem. Soc. 126 (2004) 8086.
- [10] S.D. Kenny, J.B. Pethica, R.G. Edgell, Surf. Sci. 524 (2003) 141.
- [11] C.F. McFadden, P.S. Cremer, A.J. Gellman, Langmuir 12 (1996) 2483.
- [12] D.S. Sholl, A. Asthagiri, T.D. Power, J. Phys. Chem. B 105 (2001) 4771.
- [13] B. Bhatia, D.S. Sholl, Angew. Chem. Int. Ed. 44 (2005) 7761.
- [14] G. Kresse, J. Furthmuller, Comp. Mater. Sci. 6 (1996) 15.
- [15] G. Kresse, J. Hafner, J. Phys.: Condens. Mat. 6 (1994) 8245.
- [16] D. Vanderbilt, Phys. Rev. B 41 (1990) 7892.
- [17] A. Pasquarello, K. Laasonen, R. Car, C. Lee, D. Vanderbilt, Phys. Rev. Lett. 69 (1992) 1982.
- [18] H. Jonsson, G. Mills, K.W. Jacobsen, in: Classical and Quantum Dynamics in Condensed Phase Simulations, World Scientific, 1998, p. 385.
- [19] G. Mills, H. Jonsson, Phys. Rev. Lett. 72 (1994) 1124.
- [20] G. Mills, H. Jonsson, G.K. Schenter, Surf. Sci. 324 (1995) 305.
- [21] K. Oura, V.G. Lifshits, A.A. Saranin, A.V. Zotov, M. Katayama, Surface Science: An Introduction, Springer, New York, 2003.
- [22] J.-L. Lin, A.V. Teplyakov, B.E. Bent, J. Phys. Chem. 100 (1996) 10721.
- [23] P.J. Feibelman, J. Hafner, G. Kresse, Phys. Rev. B 58 (1998) 2179.
- [24] A. Ahmadi, G. Attard, J. Feliu, A. Rodes, Langmuir 15 (1999) 2420.
- [25] Z. Sljivancanin, K.V. Gothelf, B. Hammer, J. Am. Chem. Soc. 124 (2002) 14789.
- [26] T. Li, B. Bhatia, D.S. Sholl, J. Chem. Phys. 121 (2004) 10241.
- [27] B. Bhatia, D.S. Sholl, J. Chem. Phys. 122 (2005) 204707.
- [28] R.B. Rankin, D.S. Sholl, J. Chem. Phys. 124 (2006) 074703.
- [29] T.D. Power, A. Asthagiri, D.S. Sholl, Langmuir 18 (2002) 3737.
- [30] M. Giesen, S. Dieluweit, J. Mol. Catal. A 216 (2004) 263.